



Coherence in the output spectrum of frequency shifted feedback lasers

L.P. Yatsenko^a, B.W. Shore^{b,*}, K. Bergmann^b

^a Institute of Physics, National Academy of Sciences of Ukraine Prospect Nauki 46, Kiev-39, 03650, Ukraine

^b Technical University, Kaiserslautern, 67653 Kaiserslautern, Germany

EXHIBIT B

ARTICLE INFO

Article history:

Received 9 June 2008

Received in revised form 30 August 2008

Accepted 1 October 2008

ABSTRACT

We present a detailed theoretical analysis, using correlation functions, of the coherence properties of the output from a frequency shifted feedback (FSF) laser seeded simultaneously by an external seed laser and by spontaneous emission (SE). We show that the output of a FSF laser is a cyclostationary process, for which the second-order correlation function is not stationary, but periodic. However, a period-averaged correlation function can be used to analyze the optical spectrum. From the fourth-order correlation function of the output of a Michelson interferometer we obtain the essential characteristics of the radio-frequency (RF) spectrum, needed for describing the use of the FSF laser for optical-ranging metrology. We show that, even for a FSF laser seeded by SE, the RF spectrum comprises a sequence of doublets, whose separation gives directly a measure of the length difference between the interferometer arms. This doublet structure is a result of the correlation of interference terms of individual components of the cyclostationary stochastic process. It is not seen in the optical spectrum of the FSF laser but is observable in the RF spectrum. We analyze the competition between SE and continuous wave (CW) seeding to obtain an analytical expression for the ratio of power in the discrete CW signal to the background continuum spectrum from SE. We show that, unlike mode competition in conventional lasers, where there occurs exponential selectivity, here there is a balance between the two fields; the power in the fields is related linearly, rather than exponentially, to the control parameters.

© 2008 Elsevier B.V. All rights reserved.

1. Introduction

The remarkable properties of frequency shifted feedback (FSF) lasers have drawn attention as broad-band light sources [1–4] and, more recently, as tools for metrology [5–9]. In essence, an FSF laser comprises a closed optical path, of total optical length L (a linear cavity or a ring), in which light undergoes not only the usual gain of energy from excited states but also, during each cavity round trip, a discrete-frequency shift Δ . This differs from the axial mode spacing of the cavity, the free-spectral range (FSR), which is $2\pi c/L$. The operation of FSF lasers has been considered by several research groups [10–20] and it has been used for a number of practical applications [21–26].

Two complementary viewpoints offer means for understanding the output characteristics, and uses, for an FSF laser. In one, the output field is regarded as a comb of chirped frequencies, separated in frequency at any instant by the free-spectral range $2\pi c/L$ (the *moving-comb model*) [5,6,14–16,27]. The other approach considers the output growing from a discrete-frequency seed as a stationary set of frequencies starting from the seed frequency

and separated from each other by Δ [19,20,23,28,29]. Spontaneous emission (SE) provides a continuous distribution of such seed frequencies.

For applications to metrology, specifically the determination of distances by optical ranging, it is important to understand the coherence characteristics of the output from an FSF laser. In the absence of any external seed, this output originates from a distribution of spontaneous-emission (SE) events within the gain medium. These are uncorrelated and intrinsically incoherent. We here examine, by following a sequence of cyclic passages within the FSF cavity, how this radiation acquires coherence properties, as evidenced in correlation functions.

We discuss here the operation of a FSF laser whose field originates either entirely from spontaneous emission or else from the joint action of spontaneous emission and a continuous-wave (CW) monochromatic laser seed. We pay particular attention to the RF spectrum of the output of a Michelson interferometer driven by a FSF laser. As we will note, this signal underlies metrology applications.

Earlier we have presented the basic theory of the operation of a FSF laser [19]. That work treated the SE as a seed field of very large bandwidth. It also described the effect of an external CW laser seed field, one whose phase could be modulated. However, it did not discuss the competition between these two sources. Here we remedy these shortcomings by treating the two sources as coexisting,

* Corresponding author. Address: 618 Escondido Cir., Livermore, CA 94550, USA.
Tel.: +1 925 455 0627.

E-mail address: bwshore@alum.mit.edu (B.W. Shore).

All applications of FSF lasers to distance measurements (optical ranging) rely on measurements of the RF spectrum of the output of a Michelson interferometer with FSF-laser input. Hitherto there has been no quantitative *ab initio* theory of the properties of this spectrum. Such a description must originate with intensity correlation functions, as presented here. We will show how the frequency-shifting element produces a field which, when passed through a Michelson interferometer, produces spectral signals from which the interferometer-arm distance can be deduced. Specifically, the information is contained in sets of frequency doublets. We present here a first-principles derivation of the “beat frequencies” that have been discussed earlier based on the moving-comb model of FSF operation. We show that such signals occur even when the FSF laser is seeded entirely by spontaneous emission, and that there is no need to invoke a moving comb model to explain this structure. The interferences from such SE sources are not seen in the optical spectrum of the FSF laser; they are observable only in the RF signals from the interferometer.

Our earlier work [19] considered the FSF output field from a specific seed field. We used these results to model the output from an FSF laser seeded either solely by SE or exclusively by an externally controlled laser field. As shown in [7], the latter option offers significant improvement in signal-to-noise ratio over SE seeding. The present paper treats FSF-laser operation when an external seed field is accompanied by the inevitable spontaneous emission that provides an unavoidable stochastic background. In normal laser operation the competition between modes leads to exponential growth of favored modes at the expense of those with less gain. We shall show that in the FSF laser the competition between SE and external seed does not act in this way. Instead, there occurs a balance between the two fields that is related linearly, rather than exponentially, to the control parameters. Although it would be desirable to suppress the amplified spontaneous emission (ASE) component of the FSF-laser output, thereby improving the signal-to-noise ratio, we shall show that this is not possible. This behavior differs, perhaps unexpectedly, from that of a normal laser, where suitable choice of gain characteristics can place all of the output into a favored mode.

2. Basic model

This article draws upon two recent papers [7,19] that present, in some detail, an idealized model for an FSF laser. We here first review the basic principles of that work and then extend it by examining correlation functions, thereby allowing analysis of the coherence and spectral properties of the FSF laser.

2.1. The FSF-laser layout

Fig. 1 presents a schematic drawing of the essentials of a FSF laser in a ring configuration. Light propagates along a closed optical path that passes through a gain medium (G), a frequency shifter

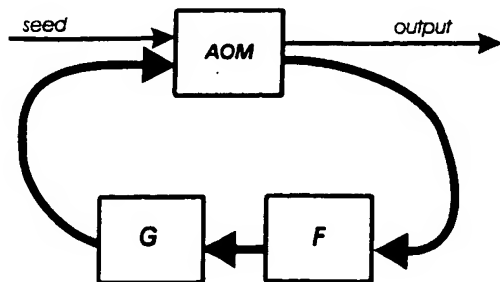


Fig. 1. Symbolic diagram of a ring cavity showing gain G, spectral filter F and frequency-shifter AOM as well as seed and output.

[usually accomplished by an acousto-optic modulator, (AOM)] and a filter (F). In G a combination of stimulated emission and spontaneous emission add energy. The AOM adds a fixed increment Δ to each frequency component. A number of elements within the overall optical path have frequency dependent losses that we here represent as a single spectral filter, F. The output emerges through the zero diffraction order of the AOM. The AOM also serves to couple any external seed laser beam into the cavity.

2.2. The field description

The filtering elements (F), which remove energy, and the gain medium (G), which replenishes this energy, together provide an *effective gain* (the growth minus the loss) distributed over a range of frequencies. We take the center of this range to be ω_f , regarding this as a carrier frequency. We consider the propagation of the electric field along a one-dimensional path, coordinate z , within the ring. The round-trip time in the cavity is $\tau_r = L/c$.

We denote by $E(t)$ the complex-valued electric field at position $z = 0$, taken to be the entrance surface of the AOM. We express this field in terms of a complex-valued envelope $\mathcal{E}(t)$ and a carrier:

$$E(t) = \mathcal{E}(t) \exp(-i\omega_f t). \quad (1)$$

The intensity of the FSF laser at $z = 0$, is

$$I(t) = \frac{c}{8\pi} |\mathcal{E}(t)|^2. \quad (2)$$

The AOM diffracts into first order a fraction of the beam intensity, denoted \mathcal{R}^2 . Typically $\mathcal{R}^2 \approx 0.9$. The frequency of this fraction is shifted, in passing through the AOM, by Δ . This portion continues to circulate within the cavity. The unshifted fraction $(1 - \mathcal{R}^2)$, usually small, remains in zeroth order and forms the output field.

We consider an arbitrary but fixed reference time T and a time window that endures for one round-trip time prior to T . Within this interval, $T - \tau_r < t < T$, we introduce a sliding windowed Fourier transform (SWFT) of the envelope, writing

$$\mathcal{E}(t) = \int_{-\infty}^{\infty} d\omega \mathcal{E}(\omega, T) \exp(-i\omega t), \quad \text{for } T - \tau_r < t < T, \quad (3)$$

where

$$\mathcal{E}(\omega, T) \equiv \frac{1}{2\pi} \int_{T-\tau_r}^T dt \mathcal{E}(t) \exp(+i\omega t). \quad (4)$$

Here and in the following we denote by $\omega \equiv \omega - \omega_f$ a frequency offset from the carrier ω_f . The SWFT field $\mathcal{E}(\omega, T)$ for a fixed reference time T provides the essential tool with which we express the operation of the FSF and the output field [19]. From it we construct the field envelope $\mathcal{E}(t)$ for all time, and deduce the output characteristics of the FSF for any given experimental conditions.

2.3. The field amplitude equations

As in our earlier work [19], we derive the basic equation for the laser field by considering its history during the round trip prior to time T . It began this circuit, starting at time $t = T - \tau_r$, with frequency $\omega = \omega_f + \omega - \Delta$. It then underwent a frequency shift Δ as it passed through the AOM. It changed amplitude in passing through the filter and gain medium. It also acquired a phase increment $(\omega_f + \omega)\tau_r$ as it propagated around the loop. To describe these changes it proves useful to introduce a two-dimensional time–frequency space $\vec{\mathcal{X}} = (\omega, T)$ in which to present the equations [19]. Successive circulations around the ring involve a change of the two-dimensional vector $\vec{\mathcal{X}}$ by the increment $\vec{\mathcal{X}}_0 = (\Delta, \tau_r)$. The field change after one round trip is expressible as

$$\mathcal{E}(\vec{\mathcal{X}}) = \mathcal{E}(\vec{\mathcal{X}} - \vec{\mathcal{X}}_0) \exp \left[G(\vec{\mathcal{X}}) \right] + \xi(\vec{\mathcal{X}}) + \mathcal{L}(\vec{\mathcal{X}}). \quad (5)$$

Here the effect of gain and loss appears through the propagator argument $G(\vec{X})$, described in detail below, and the terms $\xi(\vec{X})$ and $\varepsilon(\vec{X})$ represent, in Fourier space, additions to the field during the time interval τ_r . The first of these, $\xi(\vec{X})$, expresses the field increment supplied by spontaneous emission. It is the SWFT of $\xi_{sp}(t)$, the amplitude of the stochastic field created by spontaneous-emission events,

$$\xi(\vec{X}) \equiv \xi(\omega, T) = \frac{1}{2\pi} \int_{T-\tau_r}^T dt \xi_{sp}(t) \exp(+i\omega t). \quad (6)$$

The second contribution to the field, $\varepsilon(\vec{X})$, describes the external seed field, if present. We take this to have a carrier frequency ω_s offset from the central filter frequency ω_f by ω_s ,

$$\omega_s = \omega_f + \omega_s. \quad (7)$$

We are interested in seeding by monochromatic light; we write its SWFT as

$$\varepsilon(\vec{X}) = \frac{\varepsilon_s}{2\pi} \int_{T-\tau_r}^T dt \exp[-i\omega_s t + i\omega t], \quad (8)$$

where ε_s is the amplitude of the seeding laser field within the cavity.

We write the propagator argument $G(\vec{X})$ as the difference between gain $g(\omega)$ and losses $f(\omega)$, modified by the phase $(\omega_f + \omega)\tau_r$, acquired during the round trip. We approximate the effect of losses by means of a filter function, taken to be a quadratic centered at $\omega = \omega_f$ with characteristic width Γ_f ,

$$f(\omega) = f_m + \frac{1}{2} \left(\frac{\omega - \omega_f}{\Gamma_f} \right)^2. \quad (9)$$

The frequency-independent term f_m describes fixed losses, such as those from mirror reflectivities.

We will regard the spectral filter as having narrower bandwidth than the broader bandwidth of the gain medium; it fixes the range of frequencies we need to consider. In this approximation we neglect the frequency dependence of the gain and approximate it as

$$g(\omega) \equiv g_{sat} = \frac{g_0}{1 + I/I_{sat}}. \quad (10)$$

Here g_{sat} is the saturated frequency-independent gain, g_0 is the unsaturated gain, I is the laser intensity averaged over one round trip and I_{sat} is the saturation intensity. The averaged intensity, and hence the saturated gain, must be evaluated from appropriate equations describing the FSF laser, see Section 5.1 below. Combining these three contributions, we write the propagator argument as

$$G(\vec{X}) \equiv G(\omega, T) = i(\omega_f + \omega)\tau_r + g_{sat} - f_m - \frac{1}{2} (\omega/\Gamma_f)^2. \quad (11)$$

This depends on frequency ω through the detuning $\omega \equiv \omega - \omega_f$.

The basic parameters under the control of the experimenter are those of the cavity τ_r , Δ , those of the filter ω_f , Γ_f , f_m , those of the gain g_0 , I_{sat} , and those of the seed, ε_s , ω_s . The mean intensity \bar{I} , and the concomitant saturated gain g_{sat} must be determined such that the equations for the field, with predicted output intensity, are self consistent.

2.4. The output intensity

An important characteristic of the FSF-laser output is the intensity averaged over a round trip,

$$\bar{I}(T) \equiv \frac{1}{\tau_r} \int_{T-\tau_r}^T dt I(t). \quad (12)$$

We define the spectral intensity $I(\omega, T)$ by writing this average as a frequency distribution,

$$\bar{I}(T) = \int_{-\infty}^{\infty} d\omega I(\omega, T). \quad (13)$$

Using Eq. (3) we write the intensity as

$$I(t) = \frac{c}{8\pi} \int_{-\infty}^{\infty} \int_{-\infty}^{\infty} d\omega_1 d\omega_2 \exp[-i(\omega_1 - \omega_2)t] \times \delta(\omega_1, T) \delta(\omega_2, T)^*. \quad (14)$$

From this integral we extract an expression for the spectral intensity of Eq. (13) as

$$I(\omega, T) = \frac{c}{8\pi} \int_{-\infty}^{\infty} d\omega' \delta(\omega, T) \delta(\omega + \omega', T)^* \times \frac{1 - \exp[-i\omega'\tau_r]}{i\omega'\tau_r} \exp[i\omega'T]. \quad (15)$$

The fields described here, and the corresponding output intensity, involve uncontrollable events, the stochastic processes that describe spontaneous emission. Observations inevitably introduce averages over stochastic realizations of the average intensity during a round trip. Thus we are interested in stochastic averages $\langle \dots \rangle$ that give the spectrum

$$J(\omega) \equiv \langle I(\omega, T) \rangle, \quad (16)$$

and the mean intensity

$$\bar{J} \equiv \langle \bar{I}(T) \rangle. \quad (17)$$

2.5. The general solution for the output field

The FSF laser based on the growth of spontaneous emission acts as a regenerative amplifier of spontaneous emission, as described by basic Eq. (5). The solution to this equation, as discussed earlier [19], is expressible as the contribution of two parts,

$$\mathcal{E}(\vec{X}) = \mathcal{E}_{sp}(\vec{X}) + \mathcal{E}_{seed}(\vec{X}), \quad (18)$$

a field that grows from the spontaneous emission,

$$\mathcal{E}_{sp}(\vec{X}) = \xi(\vec{X}) + \sum_{n=1}^{\infty} \xi(\vec{X} - n\vec{X}_0) \exp[\lambda_n(\vec{X})], \quad (19)$$

and a field that grows from the external seed,

$$\mathcal{E}_{seed}(\vec{X}) = \varepsilon(\vec{X}) + \sum_{n=1}^{\infty} \varepsilon(\vec{X} - n\vec{X}_0) \exp[\lambda_n(\vec{X})]. \quad (20)$$

Here

$$\lambda_n(\vec{X}) \equiv \sum_{l=0}^{n-1} G(\vec{X} - l\vec{X}_0). \quad (21)$$

These formulas express the field as the most recent added increments from seed and spontaneous emission, together with the succession of fields from earlier passes, each altered by the appropriate propagator $\exp[\lambda_n(\vec{X})]$. Our earlier work considered each of these separately. Here we consider the operation of the laser when both are present.

3. Seeding by spontaneous emission. The optical spectrum

Earlier work on the theory of the FSF laser emphasized the structure of the output fields. To gain a full understanding of the FSF laser it is necessary to evaluate various spectral properties. For the field emerging from the FSF cavity the significant observable is the optical spectrum. When the FSF laser is used for metrology, the significant observable is the RF spectrum from a Michelson interferometer. To quantify either of these it is necessary to have a theoretical description of various correlation

functions. Specifically, we require the second-order correlation functions for the optical spectrum, considered in this section. We require fourth-order functions to describe the RF spectrum, discussed in Section 4.

We begin by considering the FSF laser seeded only by SE. This provides a simple foundation for more elaborate models of FSF-laser operation.

3.1. Passive frequency-independent cavity

To simplify the problem as much as possible, we first consider a passive-cavity model, one in which there is no gain and in which losses are independent of frequency. We assume that the cavity field originates with the intracavity spontaneous emission. The lack of frequency dependence allows us to construct the solution using the fact that after one round trip the field $E(t)$ reproduces, with no distortion, the field at the earlier time $t - \tau_r$. The results of this simplified approach clarify some of the apparent peculiarities of the FSF-laser field.

For our idealized cavity the main losses occur from the small nonideality of the AOM, whose efficiency $\mathcal{R}^2 = \exp(-2f_m) < 1$ is taken here to be independent of frequency. We assume that the spontaneous emission source in the cavity creates the stochastic electric field with the amplitude $\xi_{sp}(t)$ and the carrier optical frequency ω_{sp} . We take $\xi_{sp}(t)$ to have mean value zero and the correlation behavior

$$\langle \xi_{sp}(t) \xi_{sp}^*(t + \tau) \rangle = \xi_0^2 F(\tau). \quad (22)$$

To avoid the unphysical occurrence of an infinite energy and infinitely broad spectrum we take the function $F(\tau)$ to be

$$F(\tau) = \frac{\Gamma_{sp}}{2} \exp(-\Gamma_{sp}|\tau| + i[\omega_{sp} - \omega_f]\tau), \quad (23)$$

rather than the usual delta function $F(\tau) = \delta(\tau)$. Here Γ_{sp} and ω_{sp} are, respectively, the spectral width and the central frequency of the spontaneous-emission line, much larger than all other frequencies in the system. (For the moment we disregard gain; the assumption of very large Γ_{sp} is equivalent to our earlier assumption of constant gain within the spectral range of interest.)

Because we assume here that the cavity losses are independent of frequency we can write the amplitude $\mathcal{E}(t)$ of the electric field in the cavity as the sum of the immediate spontaneous-emission contribution $\xi_{sp}(t)$ together with emission that was present at the earlier time $t - \tau_r$ along with similar emissions at a succession of earlier times, each diminished by a diffraction \mathcal{R} but with unchanged time dependence,

$$\begin{aligned} \mathcal{E}(t) = & \xi_{sp}(t) + \mathcal{R}\xi_{sp}(t - \tau_r)e^{-i\Delta t} + \mathcal{R}^2\xi_{sp}(t - 2\tau_r)e^{-i\Delta(t - \tau_r)t - i\Delta t} \\ & + \mathcal{R}^3\xi_{sp}(t - 3\tau_r)e^{-i\Delta(t - 2\tau_r)t - i\Delta(t - \tau_r)t - i\Delta t} + \dots \end{aligned} \quad (24)$$

Thus the cavity field is an infinite sum

$$\mathcal{E}(t) = \xi_{sp}(t) + \sum_{n=1}^{\infty} \mathcal{R}^n \xi_{sp}(t - n\tau_r) e^{-in\Delta t + i\Phi_n} \quad (25)$$

where the phase of component n is $\Phi_n = \sum_{l=0}^{n-1} l\Delta\tau_r$.

We infer from Eq. (25) that the spectrum of the field is the sum of spontaneous-emission spectra weighted with \mathcal{R}^{2n} and shifted by $n\Delta$. We verify this by examining the second-order correlation function for the electric field amplitude,

$$G^{(2)}(t, t + \tau) = \langle \mathcal{E}(t) \mathcal{E}^*(t + \tau) \rangle \exp(i\omega_f \tau). \quad (26)$$

The term $\exp(i\omega_f \tau)$ provides a shift to the optical frequency.

It is customary to deal with stationary processes for which correlation functions depend on the time interval τ but not on the time t . For such processes one can evaluate the power spectrum

as the Fourier transform of the correlation function; that is the content of the Wiener-Khinchine (WK) theorem. For the system considered here this theorem does not apply. Instead, we use Eq. (25) and the correlation behavior of the spontaneous-emission source, Eq. (22), to obtain the result

$$G^{(2)}(t, t + \tau) = \xi_0^2 \sum_{n,k=0}^{\infty} \mathcal{R}^{n+k} F(\tau - [n - k]\tau_r) \times \exp[iS(t, n, k) + i\omega_{sp}\tau] \quad (27)$$

where

$$S(t, n, k) \equiv -(n - k)\Delta t + k\Delta\tau + \Phi_n - \Phi_k. \quad (28)$$

This correlation function $G^{(2)}(t, t + \tau)$ depends explicitly on time t . This means that the electric field in the FSF laser is not a stationary process. However, this time dependence is periodic, with period $2\pi/\Delta$. Thus we have here an example of a stochastic process which is periodically correlated (or *cyclostationary*, *periodically stationary* [30]). For such a process the spectrum can be defined as the output of a narrow-bandwidth optical filter. The output of such a filter, for such a process, is obtained from the Fourier transform of the period-averaged correlation function [30]. When we average over time the terms of Eq. (27) with $k \neq n$ cancel, leading to the result

$$g^{(2)}(\tau) \equiv \overline{G^{(2)}(t, t + \tau)} = \xi_0^2 \sum_{k=0}^{\infty} \mathcal{R}^{2k} F(\tau) e^{ik\Delta\tau + i\omega_{sp}\tau}. \quad (29)$$

The laser spectrum is the Fourier transform of this time-averaged correlation function,

$$J^{(2)}(\omega) = \frac{c}{4\pi} \frac{1}{2\pi} \int_{-\infty}^{\infty} d\tau g^{(2)}(\tau) \exp(-i\omega\tau). \quad (30)$$

This can be considered as an extension of the WK theorem to cyclostationary processes.

Because the correlation function $g^{(2)}(\tau)$ is the sum of independent terms, so too is the spectrum the sum of separate spectra.

$$\mathcal{L}_{spont}(\omega) = \frac{c}{4\pi} \frac{\xi_0^2}{2\pi} \int_{-\infty}^{\infty} d\tau F(\tau) e^{i\omega_{sp}\tau - i\omega\tau}, \quad (31)$$

each offset by an increment Δ and weighted by a power of \mathcal{R}^2 ,

$$J^{(2)}(\omega) = \sum_{k=0}^{\infty} \mathcal{R}^{2k} \mathcal{L}_{spont}(\omega - \omega_{sp} - k\Delta). \quad (32)$$

This result confirms our expectation based upon Eq. (25).

3.2. Frequency-dependent effective gain

We next consider a more realistic model of the FSF laser by including gain and frequency-dependent losses. The field is given by Eq. (19). We assume that the width Γ_{sp} of the spontaneous-emission spectrum is much larger than the width Γ_f of the intracavity filter. Thus, the spontaneous-emission process $\xi_{sp}(t)$ can be considered here as a delta-correlated (Wiener-Levy) stochastic process:

$$\langle \xi_{sp}(t_1) \xi_{sp}^*(t_2) \rangle = \xi_0^2 \delta(t_1 - t_2). \quad (33)$$

When we use this property of $\xi_{sp}(t)$ to calculate the field, using Eq. (19) we obtain the correlation function

$$\begin{aligned} G^{(2)}(t, t + \tau) = & \frac{\xi_0^2}{(2\pi)} \int_{-\infty}^{\infty} d\omega \sum_{n=0}^{\infty} \\ & \times \exp \left[\sum_{l=0}^{n-1} [g_{sat} - f(\omega - l\Delta)] + \sum_{l=0}^{n+M-1} [g_{sat} - f(\omega - l\Delta)] \right] \\ & \times \exp \left[i(\omega + \omega_f)\delta\tau + iM\Delta t + \frac{i}{2}\Delta M^2\tau_r - \frac{i}{2}\Delta M\tau_r \right]. \end{aligned} \quad (34)$$

We have here defined M and $\delta\tau$ by expressing τ as $\tau = M\tau_r + \delta\tau$ with $-\tau_r/2 < \delta\tau < \tau_r/2$.

As in a passive FSF cavity, the correlation function $G^{(2)}(t, t + \tau)$ given by Eq. (34) depends explicitly on time t . As discussed above, to obtain the spectrum we need the period-averaged correlation function. When we average over time the terms of Eq. (34) with $M \neq 0$ cancel. The resulting average vanishes unless $-\tau_r/2 < \tau < \tau_r/2$, when it gives the result

$$g^{(2)}(\tau) = \frac{\xi_0^2}{(2\pi)} \int_{-\infty}^{\infty} d\omega \sum_{n=0}^{\infty} \exp[S_n + i(\omega + \omega_f)\tau]. \quad (35)$$

The amplitude of component n here depends on the exponent

$$S_n \equiv 2 \sum_{l=0}^{n-1} [g_{sat} - f(\omega - l\Delta)]. \quad (36)$$

Because the spectral width of $J(\omega)$ is much larger than $2\pi/\tau_r$, this averaged correlation function is just the Fourier transform of the spectral density,

$$\frac{c}{8\pi} g^{(2)}(\tau) = \int_{-\infty}^{\infty} d\omega J^{(2)}(\omega) \exp[i(\omega + \omega_f)\tau], \quad (37)$$

with

$$J^{(2)}(\omega) = \frac{c}{8\pi} \frac{\xi_0^2}{(2\pi)} \sum_{n=0}^{\infty} \exp(S_n). \quad (38)$$

This result was obtained earlier [19] using the definition (15) of the optical spectral density.

4. Seeding by spontaneous emission. The radio-frequency spectrum

As we have shown above, the FSF laser output is an example of a cyclostationary stochastic process [30]. This property has no substantial consequences for the second-order correlation functions, such as those associated with the optical spectrum, other than the need to average over a period. However, the cyclostationarity has significant consequences in the fourth-order correlation functions. These determine, for example, the RF spectrum of the FSF output intensity. In this section we analyze such signals.

4.1. Passive, frequency-independent cavity

The output intensity of the idealized FSF cavity, seeded only by spontaneous emission, will obviously be noisy. The RF spectrum of the fluctuations of the output intensity is of special interest for applications to metrology, where it is observed the output of a Michelson interferometer. Observations of the RF spectrum were important in the use by Nakamura et al. of a FSF laser, not seeded from an external source, for ranging measurements [5,6]. RF spectral measurements continue to be central to the use of externally seeded FSF lasers for ranging [9].

The RF spectrum derives from the second-order correlation function of the intensity, i.e. the fourth-order correlation function of the electric field of Eq. (25). The intensity is

$$\begin{aligned} I(t) &= \frac{c}{8\pi} \mathcal{E}(t) \mathcal{E}^*(t) \\ &= \frac{c}{8\pi} \sum_{n,k=0}^{\infty} \mathcal{R}^{n+k} \xi_{sp}(t - n\tau_r) \xi_{sp}^*(t - k\tau_r) \times e^{i(n-k)\Delta t - i\Phi_n + i\Phi_k}. \end{aligned} \quad (39)$$

We define the correlation function for this intensity, based on deviation from the mean value \bar{I} , as

$$G^{(4)}(t, \tau) = \langle [I(t) - \bar{I}][I(t + \tau) - \bar{I}] \rangle = \langle I(t)I(t + \tau) \rangle - \bar{I}^2. \quad (40)$$

We express the averages as the multiple sums

$$\begin{aligned} \langle I(t)I(t + \tau) \rangle &= (c/8\pi)^2 \sum_{n,k,m,s=0}^{\infty} \mathcal{R}^{n+k} \mathcal{R}^{m+s} \\ &\times \langle \xi_{sp}(t - n\tau_r) \xi_{sp}^*(t - k\tau_r) \xi_{sp}(t + \tau - m\tau_r) \xi_{sp}^*(t + \tau - s\tau_r) \rangle \\ &\times \exp[i(n - k)\Delta t + i(m - s)\Delta(t + \tau) - i\Phi_n + i\Phi_k - i\Phi_m + i\Phi_s] \end{aligned} \quad (41)$$

and

$$\bar{I}^2 = (c/8\pi)^2 \left[\sum_{n,k=0}^{\infty} \mathcal{R}^{n+k} \langle \xi_{sp}(t - n\tau_r) \xi_{sp}^*(t - k\tau_r) \rangle e^{i(n-k)\Delta t - i\Phi_n + i\Phi_k} \right]^2. \quad (42)$$

To average the product of four random functions we need to invoke additional assumptions about the statistical behavior of the function $\xi_{sp}(t)$. We will assume that this is a Gaussian random process [31]. This assumption allows the factorization

$$\begin{aligned} \langle \xi_{sp}(t_1) \xi_{sp}^*(t_2) \xi_{sp}(t_3) \xi_{sp}^*(t_4) \rangle &= \langle \xi_{sp}(t_1) \xi_{sp}^*(t_2) \rangle \langle \xi_{sp}(t_3) \xi_{sp}^*(t_4) \rangle \\ &+ \langle \xi_{sp}(t_1) \xi_{sp}^*(t_4) \rangle \langle \xi_{sp}(t_3) \xi_{sp}^*(t_2) \rangle. \end{aligned} \quad (43)$$

The width of the spontaneous-emission spectral distribution is much larger than all the relevant frequency parameters. Therefore we assume that the τ dependence of the function $F(\tau)$ in Eq. (23) is much more localized than are the variations with τ in Eq. (41). We carry out the ensemble average of the particular products shown above and find that the fourth-order correlation function is independent of time:

$$G^{(4)}(t, \tau) = G^{(4)}(\tau) = G_0 \sum_{M=-\infty}^{\infty} |F(\tau - M\tau_r)|^2 \mathcal{R}^{2|M|} \quad (44)$$

with

$$G_0 = \left(\frac{c}{8\pi} \xi_0^2 \sum_{k=0}^{\infty} \mathcal{R}^{2k} \right)^2. \quad (45)$$

This correlation function does not depend on the frequency shift Δ . Therefore particular characteristics of the FSF behavior is not important; we obtain the same result by considering a cavity that has no frequency shifter. The periodic structure of the correlation functions occur because the field repeats itself after one round trip. The field at any time results builds on superpositions of many contributions, each shifted in time by τ_r , and weighted by the reflection coefficient \mathcal{R} . The interference terms involving different components do not contribute to the mean intensity but they do give important contributions to the correlation function. This correlation function is independent of time and so, by the WK theorem, the RF spectrum $J^{(4)}(\Omega)$ is its Fourier transform,

$$J^{(4)}(\Omega) = \frac{1}{2\pi} \int_{-\infty}^{\infty} d\tau G^{(4)}(\tau) \exp(-i\Omega\tau). \quad (46)$$

Thus the spectrum of output intensity fluctuations is the infinite sum

$$J^{(4)}(\Omega) = \frac{G_0}{2\pi} \int_{-\infty}^{\infty} d\tau \exp(-i\Omega\tau) \sum_{M=-\infty}^{\infty} |F(\tau - M\tau_r)|^2 \mathcal{R}^{2|M|}. \quad (47)$$

We write this as the product of a scaling factor G_0 and two frequency-dependent functions,

$$J^{(4)}(\Omega) = G_0 L_{sp}(\Omega) \mathcal{L}(\Omega). \quad (48)$$

Here the smooth envelope

$$L_{sp}(\Omega) = \frac{1}{2\pi} \int_{-\infty}^{\infty} d\tau |F(\tau)|^2 \exp(-i\Omega\tau) = \frac{1}{2\pi} \frac{\Gamma_{sp}/4}{1 + (\Omega/4\Gamma_{sp})^2} \quad (49)$$

incorporates the broad but finite width of the spontaneous-emission spectrum. For the RF spectrum it suffices to use the approximation $L_{sp}(\Omega) \approx L_{sp}(0) = \Gamma_{sp}/8\pi$. The sum over M in the spectrum (47) produces the factor

$$\mathcal{L}(\Omega) \equiv \sum_{M=-\infty}^{\infty} \mathcal{A}^{2|M|} \exp(-i\Omega M\tau_r) = \frac{1 - \mathcal{A}^4}{1 - 2\mathcal{A}^2 \cos \Omega\tau_r + \mathcal{A}^4}. \quad (50)$$

This is a periodic function of Ω with a period $2\pi/\tau_r$. For a high quality cavity, one with $1 - \mathcal{A}^2 \ll 1$, this function describes a set of narrow lines, each centered near a value $\Omega_q = 2\pi q/\tau_r$ for some positive integer q . The line profile $\mathcal{L}(\Omega - \Omega_q)$ of each individual component is a Lorentzian

$$\mathcal{L}(x) = \frac{1}{(1 - \mathcal{A})[1 + (x/\Gamma_c)^2]}, \quad (51)$$

where $\Gamma_c = 2(1 - \mathcal{A})/\tau_r$.

Thus the RF spectrum of the passive cavity output comprises a sequence of equidistant spectral features, each with the same narrow profile $\mathcal{L}(x)$, and each centered at an integer multiple of the cavity axial-mode frequency-difference $2\pi/\tau_r$. The width of each peak is determined by the lifetime of a photon in the cavity. The amplitudes of the peaks differ very little. The origin of this spectrum regularity is a periodic repetition of any initial fluctuation of the spontaneous emission source. Note, as remarked above, that the FSF behavior of the cavity has no effect on these properties of the RF spectrum.

Frames (a) and (d) of Fig. 2 illustrate the properties of the correlation function $G_1(\tau)$ of Eq. (44) and the spectrum $S(\Omega)$ of Eq. (47). For this figure the various times have been chosen to illustrate the essential physics rather than to describe any actual realization. The individual peaks of frame (a) have widths set by the atomic spontaneous emission lifetime; in practice those widths would be much less than the spacing, and the figure would show only vertical lines. The dashed-line envelope has a decay time set by the lifetime of a photon in the cavity; in practice this decay would be much more gradual than is shown. The spectral properties of frame (d) are similarly exaggerated. The widths of the indi-

vidual peaks are set by the cavity decay time, while the dashed-line envelope expresses the spontaneous-emission lifetime.

4.2. Michelson interferometer with input from a passive cavity

Here we analyze the RF spectrum of the output of Michelson interferometer. For simplicity we consider the interferometer formed by an ideal beam splitter and two totally reflecting mirrors. We take the difference of interferometer arms to be the distance $L = cT/2$, where T is a total time delay.

The electric field in the output arm is

$$\mathcal{E}_{Mich}(t) = \frac{1}{2}[\mathcal{E}(t) + \mathcal{E}(t - T)]. \quad (52)$$

The interferometer output intensity,

$$I_{Mich}(t) = \frac{c}{32\pi} |\mathcal{E}(t) + \mathcal{E}(t - T)|^2, \quad (53)$$

can be written as a sum

$$I_{Mich}(t) = \frac{1}{4}[I(t) + I(t - T) + I_{int}(t, t - T)], \quad (54)$$

where $I(t)$ is the output intensity given by Eq. (39). The interference term

$$I_{int}(t, t - T) = 2\Re[\mathcal{E}(t)\mathcal{E}^*(t - T)] \quad (55)$$

makes no contribution to the mean intensity but, as we will show, it has important effects on the RF spectrum of the Michelson-interferometer output. The correlation function for the intensity of Eq. (54),

$$G_{Mich}^{(4)}(t, \tau) = \langle I_{Mich}(t)I_{Mich}(t + \tau) \rangle - \bar{I}_{Mich}^2 \quad (56)$$

has two distinct contributions, which we denote as $G_{Mich}^{(4)}(t, \tau) = G_3^{(4)}(t, \tau) + G_{int}^{(4)}(t, \tau)$. The first of these is the sum of three individual correlation functions

$$G_3^{(4)}(t, \tau) \equiv G_3^{(4)}(\tau) = \frac{1}{16} [2G^{(4)}(\tau) + G^{(4)}(\tau + T) + G^{(4)}(\tau - T)], \quad (57)$$

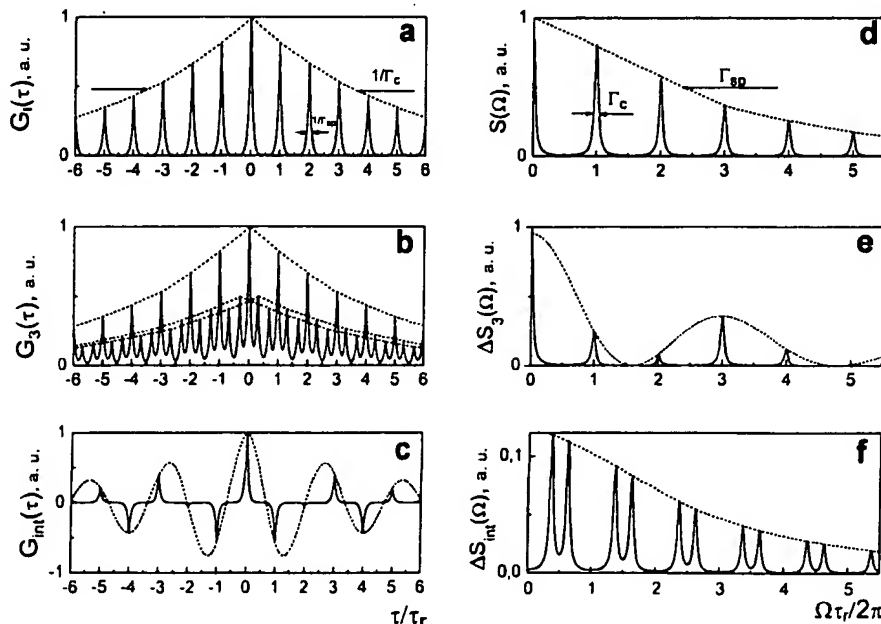


Fig. 2. Left-hand frames (a), (b), (c) show the correlation function, right-hand frames (d), (e), (f) show the resulting spectrum. Top row, frames (a) and (b) show the second-order correlation function of Eq. (44) and the corresponding optical spectrum of Eq. (47). Middle row, frames (b) and (e) show the correlation function $G_3^{(4)}$ of Eq. (57) and the corresponding RF spectrum $J_3^{(4)}$ of Eq. (62). Bottom row, frames (c) and (d) show the correlation function $G_{int}^{(4)}$ of Eq. (58) and the corresponding RF spectrum $J_{int}^{(4)}$ of Eq. (64). The observable spectrum is the sum of contributions (e) and (f).

and is independent of time. The second part originates with the interference intensities,

$$G_{int}^{(4)}(t, \tau) = \frac{1}{16} \langle I_{int}(t, t - T) I_{int}(t + \tau, t + \tau - T) \rangle. \quad (58)$$

This interference term can be averaged in the same way as was done when obtaining $G^{(4)}(\tau)$ in the previous subsection. The result is

$$G_{int}^{(4)}(t, \tau) = G_{int}^{(4)}(\tau) = G_0 \sum_{M=-\infty}^{\infty} F(\tau - M\tau_r)^2 \mathcal{A}^{2|M|} \cos[M\Delta T]. \quad (59)$$

The additional phase shift ΔT between consecutive components in the cavity leads to some modulation of the correlation function with a period $2\pi\tau_r/\Delta T$.

The RF spectrum of the output from the interferometer receives contributions from two parts, corresponding to the two parts of the correlation function,

$$J_{Mich}^{(4)}(\Omega) = J_3^{(4)}(\Omega) + J_{int}^{(4)}(\Omega). \quad (60)$$

The contribution $J_3^{(4)}(\Omega)$ comprises a sequence of equidistant spectral profiles, each with the same profile $\mathcal{L}(\Omega)$ but with different amplitude:

$$\begin{aligned} J_{int}^{(4)}(\Omega) &= \frac{1}{32\pi} \\ &\times \int_{-\infty}^{\infty} d\tau [2G^{(4)}(\tau) + G^{(4)}(\tau + T) + G^{(4)}(\tau - T)] \exp(-i\Omega\tau) \\ &= \frac{G_0}{32\pi} \sum_{M=-\infty}^{\infty} \mathcal{A}^{2|M|} \int_{-\infty}^{\infty} d\tau \exp(-i\Omega\tau) \\ &\times [2F(\tau - M\tau_r)^2 + F(\tau + T - M\tau_r)^2 + F(\tau - T - M\tau_r)^2]. \end{aligned} \quad (61)$$

This function is expressible as the product of a scaling factor and three frequency-dependent functions [in contrast with the two functions of Eq. (48)],

$$J_3^{(4)}(\Omega) = \frac{G_0}{4} L_{sp}(\Omega) \mathcal{L}(\Omega) \cos^2(\Omega T/2). \quad (62)$$

The first factor, $L_{sp}(\Omega)$, can be considered constant, in keeping with our assumption of large Γ_{sp} . The second factor, $\mathcal{L}(\Omega)$, is that of Eq. (48): it describes a set of narrow peaks, centered at the discrete frequencies $\Omega_q = 2\pi q/\tau_r$. In contrast to the previous section, here there occurs an additional frequency dependence: amplitudes of the narrow discrete components are weighted by the factor $\cos^2(\Omega T/2)$, evaluated at Ω_q . This revision occurs because the correlation function G_3 originates from an incoherent sum of three components delayed by time T . Fig. 2b illustrates the properties of the correlation function $G_3^{(4)}(\tau)$ of Eq. (57) and of the spectrum $J_3^{(4)}(\Omega)$ of Eq. (62). The latter exhibits an overall damped cosine modulation, as expected.

The contribution $J_{int}^{(4)}(\Omega)$ to the RF spectrum from $G_{int}^{(4)}$, discussed next, is qualitatively different. From the definition we obtain the expression

$$\begin{aligned} J_{int}^{(4)}(\Omega) &= \frac{1}{32\pi} \int_{-\infty}^{\infty} d\tau G_0 \sum_{M=-\infty}^{\infty} F(\tau - M\tau_r)^2 \mathcal{A}^{2|M|} \cos[M\Delta T] \exp(-i\Omega\tau) \\ &= \frac{G_0}{16} L_{sp}(\Omega) \sum_{M=-\infty}^{\infty} \mathcal{A}^{2|M|} \cos[M\Delta T] \exp(iM\Omega\tau_r). \end{aligned} \quad (63)$$

This spectral function therefore comprises a set of doublets,

$$\begin{aligned} J_{int}^{(4)}(\Omega) &= \sum_{q=-\infty}^{\infty} \left[\frac{G_0}{32} L_{sp}(\Omega) \mathcal{L}(\Omega - 2\pi q/\tau_r - \gamma_c T) \right. \\ &\quad \left. + \frac{G_0}{32} L_{sp}(\Omega) \mathcal{L}(\Omega - 2\pi q/\tau_r + \gamma_c T) \right]. \end{aligned} \quad (64)$$

Fig. 2f illustrates this spectral structure. The quantity $\gamma_c = \Delta/\tau_r$, appearing here is recognizable as the chirp rate used for optical ranging.

To summarize: the total RF spectrum of the Michelson-interferometer output consists of narrow discrete components centered at the frequencies $\Omega_q = 2\pi q/\tau_r$, each weighted by a factor $\cos^2(\Omega_q T/2)$. Each of these components is accompanied by a doublet of components shifted from Ω_q by $\pm\gamma_c T$ and whose amplitudes are almost independent of q . The frequency separation of these doublets incorporates information about the difference in length $cT/2$ of the interferometer arms that are used in ranging applications of FSF lasers [5–9]. Fig. 2 illustrates, on the third line of frames, these features.

It is worth noting that the existence in the RF spectrum of components shifted by $\pm\gamma_c T$ is readily understood from a model of a FSF laser seeded by a phase fluctuating CW laser [7]. Here we see that these components appear in a model of the passive FSF cavity seeded by uncorrelated spontaneous emission as a result of interference of cyclostationary stochastic processes.

4.3. Interferometer input from a frequency-dependent cavity

Here we consider a more realistic model of the FSF laser by including both gain and frequency-dependent losses. The field is given by Eq. (19). We will continue with assumptions made in Section 3.2: the width Γ_{sp} of the spontaneous-emission spectrum is much larger than the width Γ_f of the intracavity filter, so we idealize the spontaneous-emission process $\xi_{sp}(t)$ as a delta-correlated stochastic process; its correlation function is given by Eq. (33). In addition, we assume that the width Γ_f is much larger than both the frequency shift Δ and the cavity axial-mode frequency-difference $2\pi/\tau_r$.

Using the solution (19) for the FSF laser field and the condition $\Gamma_f \gg \Delta, 2\pi/\tau_r$, we obtain, after some complicated but straightforward algebra, the following expression for the intensity correlation function $G^{(4)}(t, \tau)$ defined by Eq. (40):

$$\begin{aligned} G^{(4)}(t, \tau) &= G^{(4)}(\tau) \\ &= \left| \frac{c}{8\pi} \xi_0^2 \int_{-\infty}^{\infty} \frac{d\omega}{2\pi} \exp(i\omega\delta\tau) \sum_{n=1}^{\infty} \exp[S(\omega, n, M)] \right|^2. \end{aligned} \quad (65)$$

Here the argument of the exponent is zero unless $0 < \tau - M\tau_r < \tau_r$, when it is

$$S(\omega, n, M) = \sum_{l=0}^{n-1} [g_{sat} - f(\omega - l\Delta)] + \sum_{l=0}^{n-1+M} [g_{sat} - f(\omega - l\Delta)]. \quad (66)$$

To simplify this expression, we use the condition $\Gamma_f \gg \Delta, 2\pi/\tau_r$ and replace the summation over n in (65) by integration. The exponent $S(\omega, n, M)$ reaches a maximum at

$$n = n_{max} \simeq \frac{\omega + \omega_M}{\Delta} + M/2,$$

with $\omega_M = \sqrt{\omega_0^2 - M^2 \Delta^2/4}$. In the Gaussian approximation justified in our earlier paper [19] the parameter $\omega_0 = \sqrt{2(g_{sat} - f_m)\Gamma_f^2}$ is the frequency shift between the maximum of the Gaussian fit to the optical spectrum $J^{(2)}(\omega) = J_0 \exp[-(\omega - \omega_0 - \omega_f)^2/\tilde{\Gamma}^2]$ and the filter frequency ω_f . As shown in [19], and justified experimentally in [20], the shift ω_0 and the width $\tilde{\Gamma}$ of the FSF-laser spectrum are related by the expression

$$\tilde{\Gamma}^2 \omega_0 = \gamma^3 \equiv (\Delta\Gamma_f^2). \quad (67)$$

Using the Gaussian approximation we then write

$$\sum_{n=1}^{\infty} \exp[S(\varpi, n, M)] \simeq A \exp[S(\varpi, n_{\max}, M)]. \quad (68)$$

The phase and amplitude occurring on the right hand side are

$$S(\varpi, n_{\max}, M) \simeq \frac{-\varpi^3 + 3\varpi_0^2\varpi + 2\varpi_0^3}{3\gamma^3} - \frac{M^2}{4M_0^2} \quad (69)$$

$$A \simeq \sqrt{\pi\gamma\tilde{\Gamma}}. \quad (70)$$

Here

$$M_0 = \tilde{\Gamma}/\Delta \gg 1 \quad (71)$$

is the effective number of round trips of a SE photon in the FSF-laser cavity. Integration over ϖ gives finally

$$G^{(4)}(\tau) = G_I \sum_{M=-\infty}^{\infty} F_I(\tau - M\tau_r)^2 \exp\left[-\frac{M^2}{4M_0^2}\right], \quad (72)$$

where

$$G_I = \frac{\pi\gamma^3}{\omega_0} \left(\frac{c}{4}\xi_0^2\right)^2 \exp\left[-\frac{8\varpi_0^3}{\gamma^3}\right] \quad (73)$$

$$F_I(\tau) = \frac{\tilde{\Gamma}}{\sqrt{2\pi}} \exp\left[-\frac{\tau^2\tilde{\Gamma}^2}{4}\right]. \quad (74)$$

The correlation function (72) is very similar to the correlation function of the output intensity of the passive FSF cavity, Eq. (44), but there are two differences:

1. When gains and losses are present the width of the narrow function $F_I(\tau)$ is determined by the reciprocal of $\tilde{\Gamma}$, the width of the optical spectrum. In the passive cavity this width is fixed by the spontaneous-emission correlation time.
2. The successive maxima of the correlation-function decrease in keeping with a Gaussian law $\exp(-M^2/M_0^2)$ with $M_0\tau_r$ equal to the effective lifetime of a photon in the active FSF cavity.

It can be shown that the same is true for the correlation function of the Michelson-interferometer output excited by the active FSF laser: the contribution $G_3^{(4)}(\tau)$ is given by Eq. (57) with $G^{(4)}(\tau)$ defined by Eq. (59) and the interference term

$$G_{int}^{(4)}(\tau) = G_I \sum_{M=-\infty}^{\infty} F_I(\tau - M\tau_r)^2 \exp\left[-\frac{M^2}{4M_0^2}\right] \cos[M\Delta T]. \quad (75)$$

Thus we conclude that the RF spectrum of the FSF laser output intensity and the Michelson-interferometer output have the same behavior as in the passive cavity. The only difference is that the amplitudes of narrow discrete components centered at the frequencies $\Omega_q = 2\pi q/\tau_r$ and $\Omega_q^{(z)} = 2\pi q/\tau_r \pm \gamma_c T$ decrease according to the Gaussian law $\exp(-\Omega^2/\tilde{\Gamma}^2)$ and the shape $\mathcal{L}(\Omega - \Omega_q)$ of each narrow component is not Lorentzian but a Gaussian:

$$\mathcal{L}(x) \propto \exp\left[-x^2/(M_0\tau_r)^2\right]. \quad (76)$$

5. FSF laser with seeding by both spontaneous emission and continuous-wave radiation

5.1. The intensity equation

We consider here an FSF laser seeded simultaneously by spontaneous emission and a monochromatic seed laser. Because there is no nonlinearity in our model (only saturation of gain by the total intensity) the laser field is the sum of two fields described by Eqs.

(19) and (20), each created by one of the sources. These sources are statistically independent and so the averaged intensity is also a sum of spontaneous and discrete spectrum intensities,

$$\bar{I} = \bar{I}_{sp} + \bar{I}_{seed}. \quad (77)$$

To evaluate the contribution of the external seed, \bar{I}_{seed} , we consider a monochromatic seed, meaning that its bandwidth is much smaller than either the axial mode spacing $2\pi/\tau_r$ or the frequency shift Δ . For such a seed the field $\mathcal{E}_{seed}(t)$ is [19]

$$\mathcal{E}_{seed}(t) = \mathcal{E}_s \sum_{n=0}^{\infty} a_n \exp[-i\Phi_n - i(\omega_s + n\Delta)t], \quad (78)$$

where

$$\Phi_n \equiv -\tau_r n[\omega_s + (n+1)\Delta/2]. \quad (79)$$

We write the constant real-valued amplitudes as $a_n = \exp[S_{seed}(\mathcal{G}_{sat}, n)]$, where

$$S_{seed}(\mathcal{G}_{sat}, n) \equiv n \left[\mathcal{G}_{sat} - f_m - \frac{6\varpi_s^2 + 6\varpi_s n\Delta + 6\varpi_s \Delta + 2n^2\Delta^2 + 3\Delta^2 n + \Delta^2}{12\Gamma_f^2} \right]. \quad (80)$$

The contribution \bar{I}_{seed} of the discrete spectrum to the mean intensity \bar{I} reads

$$\bar{I}_{seed} = \frac{c}{8\pi} \overline{|\mathcal{E}_{seed}(t)|^2} = I_{seed} \sum_{n=0}^{\infty} |a_n|^2 = I_{seed} F_{seed}(\mathcal{G}_{sat}), \quad (81)$$

where the intensity of the seed laser radiation injected into the FSF laser cavity is

$$I_{seed} = \frac{c}{8\pi} |\mathcal{E}_s|^2 \quad (82)$$

and

$$F_{seed}(\mathcal{G}_{sat}) = \sum_{n=0}^{\infty} \exp[2S_{seed}(\mathcal{G}_{sat}, n)]. \quad (83)$$

The mean intensity of the spontaneous-emission spectrum,

$$\bar{I}_{sp} = \frac{c}{8\pi} \overline{|\mathcal{E}_{sp}(t)|^2} \quad (84)$$

has been evaluated earlier [19]. It can be written as

$$\bar{I}_{sp} = I_{sp} F_{sp}(\mathcal{G}_{sat}). \quad (85)$$

Here

$$I_{sp} \equiv \frac{c\Gamma_f\epsilon_0^2}{8\pi^2} \quad (86)$$

is the intensity of spontaneous emission within the spectral interval Γ_f and

$$F_{sp}(\mathcal{G}_{sat}) \equiv \frac{\pi^{1/2}}{2} \sum_{n=1}^{\infty} \exp[S_{sp}(\mathcal{G}_{sat}, n)], \quad (87)$$

with

$$S_{sp}(\mathcal{G}_{sat}, n) = n \left[2(\mathcal{G}_{sat} - f_m) - \frac{\Delta^2}{12\Gamma_f^2} (n^2 - 1) \right] - \ln(n)/2. \quad (88)$$

Because the stochastic averaging removes any interference contribution the sum of the two terms (81) and (85) gives the total intensity \bar{I} . It is this intensity that saturates the gain $\mathcal{G}_{sat} = g_0/(1 + \bar{I}/I_{sat})$. The determination of $\bar{I} = I_{sat}(\frac{g_0}{\mathcal{G}_{sat}} - 1)$ requires the solution of the following transcendental equation for \mathcal{G}_{sat} :

$$\frac{I_{sp}}{I_{sat}} F_{sp}(\mathcal{G}_{sat}) + \frac{I_{seed}}{I_{sat}} F_{seed}(\mathcal{G}_{sat}) = \left(\frac{g_0}{\mathcal{G}_{sat}} - 1 \right). \quad (89)$$

Our interest is with FSF lasers in which the output spectrum is both smooth and broad. Such conditions are possible if $I_0 \ll I_{\text{sat}}(\eta - 1)$ and if the spectral filter is sufficiently broad, $\Gamma_f \gg \Delta$. For these conditions the general operation of the FSF laser is readily understood from Fig. 3. The figure shows the cavity gain as a constant, and the loss as varying around the central frequency. The frequency shifter displaces any seed frequency toward the right. By contrast to the operation of a conventional laser, there exists a finite band of frequencies $\omega_f - \omega_0 < \omega < \omega_f + \omega_0$, symmetrically centered about the central frequency of the filter ω_f , where the frequency-dependent effective gain is positive, $g_{\text{sat}} - f_m - \frac{\omega_0^2}{2\gamma^3} > 0$. Any frequency component within this band will undergo growth as successive round trips increase the frequency by Δ . However, once the frequency exceeds $\omega_f + \omega_0$ the losses dominate, and the frequency component will diminish as further frequency shifts occur. Thus we expect the saturated gain g_{sat} to be slightly greater than the minimum loss, f_m .

To proceed we make two approximations. First, because we expect the saturated gain g_{sat} to be slightly greater than f_m we approximate it as $g_{\text{sat}} = f_m$ on the right hand side of Eq. (89). Second, as in our earlier work [19], we assume that the seed frequency is far from the central frequency of the laser spectrum, so that the laser output spectrum is very close to a Gaussian form.

We express $S_{\text{sp}}(g_{\text{sat}}, n)$ and $S_{\text{seed}}(g_{\text{sat}}, n)$ as a Taylor series, centered around the value $n = n_i$, where $dS_i(n)/dt = 0$ ($i \equiv \text{sp}$ or $i \equiv \text{seed}$), and we retain only terms through second order in $(n - n_i)$. Within this Gaussian approximation the number of discrete components in the interval ω_0 is large, $\omega_0/\Delta \gg 1$, and so we replace the summation over n in Eqs. (83) and (87) by an integration. We thereby obtain the results

$$F_{\text{seed}} \simeq \sqrt{\pi} M_0 \exp \left[\frac{2\omega_0^3 + \omega_s^3 - 3\omega_s\omega_0^2}{3\gamma^3} \right] \quad (90)$$

and

$$F_{\text{sp}} = \frac{\pi}{2} \frac{\Gamma_f}{\omega_0} \exp \left[\frac{4\omega_0^3}{3\gamma^3} \right]. \quad (91)$$

Eq. (89) now reads

$$\frac{\gamma}{\omega_0} \exp \left[\frac{4\omega_0^3}{3\gamma^3} \right] + \epsilon \sqrt{\frac{\gamma}{\omega_0}} \exp \left[\frac{2\omega_0^3 + \omega_s^3 - 3\omega_s\omega_0^2}{3\gamma^3} \right] = \frac{1}{\beta}. \quad (92)$$

Here the small parameter β , defined as

$$\beta \equiv \frac{\pi}{2} \frac{I_0 \Gamma_f}{I_{\text{sat}}(\eta - 1) \gamma}, \quad (93)$$

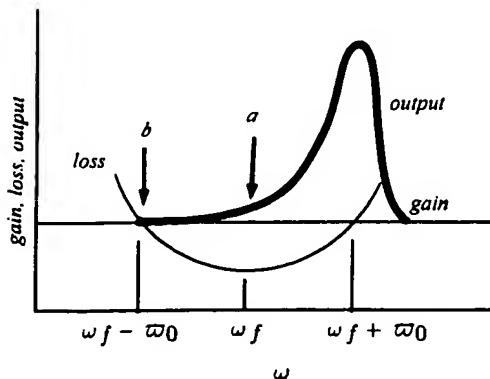


Fig. 3. Qualitative portrait of the magnitude of the FSF laser output-field spectral-density as a function of frequency, together with frequency dependence of the gain (constant) and loss (quadratic). Two choices of seed frequency are marked.

describes the spontaneous-emission source. The parameter

$$\epsilon \equiv \frac{2}{\sqrt{\pi}} \frac{\Gamma_f I_c}{\gamma I_0}, \quad (94)$$

expressing the relative importance of the seed laser, is the ratio of the intensity of the seed laser to the spontaneous-emission intensity in the spectral interval $\sqrt{\pi}\gamma/2$. Using experimental data [20] we estimate that for an Yb^{3+} -fiber laser the parameter ϵ is equal to 1 when the power of the seed laser injected into the FSF cavity is about 50 μW .

5.2. Competition between spontaneous emission and continuous-wave seeding

In this subsection we discuss solutions to Eq. (92). We consider two specific choices for the seed frequency. In the first, marked *a* in Fig. 3, the seed frequency is at the minimum of the loss curve, $\omega_s = 0$. In the second, marked *b* in the figure, the seed is near the frequency where growth first becomes possible.

5.2.1. Resonant seed, $\omega_s = \omega_f$

When the seed frequency coincides with the minimum of losses, $\omega_s = 0$, Eq. (92) takes the form of a quadratic equation

$$Y^2 + \epsilon Y = \frac{1}{\beta} \quad (95)$$

involving the variable

$$Y = \sqrt{\frac{\gamma}{\omega_0}} \exp \left[\frac{2\omega_0^3}{3\gamma^3} \right]. \quad (96)$$

From the solution,

$$Y = \frac{2/\beta}{\epsilon + \sqrt{\epsilon^2 + 4/\beta}}, \quad (97)$$

we obtain the intensity of the continuous spectrum I_{sp} as

$$I_{\text{sp}} = \frac{4/\beta}{[\epsilon + \sqrt{\epsilon^2 + 4/\beta}]^2} I_{\text{sat}}(\eta - 1) \quad (98)$$

and the intensity of the discrete spectrum as

$$I_{\text{seed}} = \frac{2\epsilon}{\epsilon + \sqrt{\epsilon^2 + 4/\beta}} I_{\text{sat}}(\eta - 1). \quad (99)$$

We see that $I_{\text{seed}} > I_{\text{sp}}$ for $\epsilon > 1/\sqrt{2\beta} \gg 1$. This is to be expected: when the seed frequency is resonant with the loss minimum, $\omega_s = \omega_f$, then the seed laser must compete with spontaneous emission that has been amplified throughout the frequency interval from $\omega_f - \omega_0$ to ω_f .

5.2.2. Seed at gain edge, $\omega_s = \omega_f - \omega_0$

A better choice for the seed laser is $\omega_s = \omega_f - \omega_0$. Eq. (92) then reads

$$\frac{\gamma}{\omega_0} \exp \left[\frac{4\omega_0^3}{3\gamma^3} \right] + \epsilon \sqrt{\frac{\gamma}{\omega_0}} \exp \left[\frac{4\omega_0^3}{3\gamma^3} \right] = \frac{1}{\beta}. \quad (100)$$

The solution to this equation for ω_0 with $\beta \ll 1$ gives the following expressions for the intensity I_{sp} of the continuous spectrum

$$I_{\text{sp}} = \frac{1}{1 + \epsilon\sqrt{\sigma}} I_{\text{sat}}(\eta - 1) \quad (101)$$

and the intensity I_{seed} of the discrete spectrum

$$I_{\text{seed}} = \frac{\epsilon\sqrt{\sigma}}{1 + \epsilon\sqrt{\sigma}} I_{\text{sat}}(\eta - 1) \quad (102)$$

where the parameter σ is defined as

$$\sigma \equiv \left(\frac{3}{4} \ln \frac{1}{\beta_{sp}} \right)^{1/3} \quad (103)$$

This parameter is almost independent of laser parameters. In previously reported experimental work [20] the measured value of σ was $\sigma \approx 2$. The discrete spectrum dominates in the case of a detuned seed laser starting with much smaller intensities: $I_{seed} > I_{sp}$ for $\epsilon > 1/\sqrt{\sigma} \sim 1$.

We see that even for optimal detuning of the seed laser there exists a large background of continuous radiation originating from spontaneous emission. For a strong seed laser, $\epsilon \gg 1$, the ratio of spontaneous to seed intensity is

$$\frac{I_{sp}}{I_{seed}} \approx \frac{1}{\epsilon \sqrt{\sigma}} \quad (104)$$

This means that, roughly speaking, the ratio of continuous to discrete spectra is equal to ratio of seed laser intensity to the intensity of spontaneous emission in the spectral interval ω_0 .

6. Summary and conclusions

We provide here the first complete theory of the spontaneous-emission seeded FSF laser based on correlation functions. We present the second-order correlation function, from which one obtains the optical spectrum of the radiation emerging from the FSF cavity. Although the correlation function is not stationary, it is periodic, and so a period-averaged correlation function leads to a simple expression for the spectrum.

We also present the fourth-order correlation function analysis with which one can evaluate the RF spectrum of the laser output intensity and of the output of a Michelson interferometer, as is used in optical-ranging metrology. We show that even in a FSF laser seeded solely by spontaneous emission this spectrum comprises a set of doublets, whose spacing gives directly a measure of the length difference between the interferometer arms. The existence of this structure in the RF spectrum of a the Michelson-interferometer output results from correlation of interference terms of individual components of a cyclostationary stochastic processes, and is not seen in the optical spectrum of the FSF laser.

We discuss the operation of a FSF laser whose field originates from the joint action of spontaneous emission and a continuous-wave monochromatic laser seed. We show that in the FSF laser the competition between SE and external seed does not act in the usual way, of exponential growth of modes with greater gain. Instead, there occurs a balance between the two fields that is related linearly, rather than exponentially, to the control parameters. Although it would be desirable to suppress the spontaneous-emission component of the FSF laser output, thereby improving the signal-to-noise ratio for optical-ranging technique based on phase

modulation of the CW seed laser, we show that this is not possible. This behavior differs from that of a normal laser.

We have not here discussed the temporal properties of the laser output. The statistical approach we have used in this paper, based on an analysis of the correlation functions and the spectral characteristics, is necessary because we consider a FSF laser seeded by spontaneous emission – a sequence of events that is completely chaotic. A time series of the laser output, just like the time series of the seeding spontaneous emission, is chaotic and conveys no information.

Acknowledgements

We acknowledge support by the Stiftung Rheinland-Pfalz für Innovation and by CNES, INTAS and NSAU (06-1000024-9075). LPY acknowledges support by the Deutsche Forschungsgemeinschaft (436-UKR-113/16).

References

- [1] F.V. Kowalski, P.D. Hale, S.J. Shattil, *Opt. Lett.* 13 (1988) 622.
- [2] I.C.M. Littler, S. Balle, K. Bergmann, *J. Opt. Soc. Am. B* 8 (1991) 1412.
- [3] I.C.M. Littler, S. Balle, K. Bergmann, *Opt. Comm.* 88 (1992) 514.
- [4] I.C.M. Littler, J.H. Eschner, *Opt. Comm.* 87 (1992) 44.
- [5] K. Nakamura, T. Miyahara, M. Yoshida, T. Hara, H. Ito, *IEEE Photonics Technol. Lett.* 10 (1998) 1772.
- [6] K. Nakamura, T. Hara, M. Yoshida, T. Miyahara, H. Ito, *IEEE J. Quant. Elect.* 36 (2000) 305.
- [7] L.P. Yatsenko, B.W. Shore, K. Bergmann, *Opt. Comm.* 242 (2004) 581.
- [8] L.P. Yatsenko, V.M. Khodakovskiy, V.V. Ogurtsov, G. Bonnet, B.W. Shore, K. Bergmann, *Proc. SPIE* 6054 (2005) 60540T.
- [9] V.V. Ogurtsov, L.P. Yatsenko, V.M. Khodakovskiy, B.W. Shore, G. Bonnet, K. Bergmann, *Opt. Comm.* 266 (2006) 266.
- [10] S. Balle, I.C.M. Littler, K. Bergmann, F.V. Kowalski, *Opt. Comm.* 102 (1993) 166.
- [11] J. Martin, Y. Zhao, S. Balle, K. Bergmann, M.P. Fewell, *Opt. Comm.* 112 (1994) 109.
- [12] F.V. Kowalski, S. Balle, I.C.M. Littler, K. Bergmann, *Opt. Eng.* 33 (1994) 1146.
- [13] S. Balle, K. Bergmann, *Opt. Comm.* 116 (1995) 136.
- [14] K. Kasahara, K. Nakamura, M. Sato, H. Ito, *Opt. Rev.* 4 (1997) 180.
- [15] K. Nakamura, F.V. Kowalski, H. Ito, *Opt. Lett.* 22 (1997) 889.
- [16] F.V. Kowalski, K. Nakamura, H. Ito, *Opt. Comm.* 147 (1998) 103.
- [17] G. Bonnet, S. Balle, Th. Kraft, K. Bergmann, *Opt. Comm.* 123 (1996) 790.
- [18] M. Stellpflug, G. Bonnet, B.W. Shore, K. Bergmann, *Opt. Express* 11 (2003) 2060.
- [19] L.P. Yatsenko, B.W. Shore, K. Bergmann, *Opt. Comm.* 236 (2004) 183.
- [20] V.V. Ogurtsov, L.P. Yatsenko, V.M. Khodakovskiy, B.W. Shore, G. Bonnet, K. Bergmann, *Opt. Comm.* 266 (2006) 627.
- [21] I.C.M. Littler, H.M. Keller, U. Gaubatz, K. Bergmann, *Zs. Physik D* 18 (1991) 307.
- [22] D.T. Mugglin, A.D. Streater, S. Balle, K. Bergmann, *Opt. Comm.* 104 (1993) 165.
- [23] J.R.M. Barr, G.Y. Liang, M.W. Phillips, *Opt. Lett.* 18 (1993) 1010.
- [24] M.J. Lim, C.I. Sukenik, T.H. Striever, P.H. Bucksbaum, R.S. Conti, *Opt. Comm.* 147 (1998) 99.
- [25] M. Cashen, V. Bretin, H. Metcalf, *J. Opt. Soc. Am. B* 17 (2000) 530.
- [26] F.V. Kowalski, C. Ndiaye, K. Nakamura, H. Ito, *Opt. Comm.* 231 (2004) 149.
- [27] A. Yoshizawa, H. Tsuchida, *Opt. Comm.* 155 (1998) 51.
- [28] M.W. Phillips, G.Y. Liang, J.R.M. Barr, *Opt. Comm.* 100 (1993) 473.
- [29] K.A. Shore, D.M. Kane, *IEEE J. Quant. Elect.* 35 (1999) 1053.
- [30] W.A. Gardner, A. Napolitano, L. Paura, *Signal Process.* 86 (2006) 639.
- [31] J.R. Klauder, E.C.G. Sudarshan, *Fundamentals of Quantum Optics*, W.A. Benjamin, Inc. New York, Amsterdam, 1968.